


ORIGINAL PAPER

Osteogenic and angiogenic profiles of the palatal process of the maxilla and the palatal process of the palatine bone

Caiyu Liao^{1,2} | Meng Lu¹ | Yuhang Hong^{1,2} | Chuanqing Mao^{1,2} | Jiangping Chen^{1,2} | Chengyan Ren^{1,2} | Minkui Lin² | Weihui Chen^{1,2} 

¹Department of Oral and Maxillofacial Surgery, Fujian Medical University Union Hospital, Fuzhou, Fujian, China

²Fujian Key Laboratory of Oral Diseases & Fujian Provincial Engineering Research Center of Oral Biomaterial & Stomatological Key Laboratory of Fujian College and University, School and Hospital of Stomatology, Fujian Medical University, Fuzhou, Fujian, China

Correspondence

Weihui Chen, Fujian Medical University Union Hospital, No. 29 Xinquan Road, Fuzhou 350001, Fujian, China.
Email: dr_whchen@yahoo.com

Funding information

The Natural Science Foundation of Fujian Province of China, Grant/Award Number: 2019J02011; The Yong and Middle-aged Teacher Project of Fujian Province Education Department, Grant/Award Number: JAT170225

Abstract

Hard palate consists anteriorly of the palatal process of the maxilla (ppmx) and posteriorly of the palatal process of the palatine (ppp). Currently, palatal osteogenesis is receiving increasing attention. This is the first study to provide an overview of the osteogenesis process of the mouse hard palate. We found that the period in which avascular mesenchymal condensation becomes a vascularized bone structure corresponds to embryonic day (E) 14.5 to E16.5 in the hard palate. The ppmx and ppp differ remarkably in morphology and molecular respects during osteogenesis. Osteoclasts in the ppmx and ppp are heterogeneous. There was a multinucleated giant osteoclast on the bone surface at the lateral-nasal side of the ppmx, while osteoclasts in the ppp were more abundant and adjacent to blood vessels but were smaller and had fewer nuclei. In addition, bone remodeling in the hard palate was asymmetric and exclusively occurred on the nasal side of the hard palate at E18.5. During angiogenesis, CD31-positive endothelial cells were initially localized in the surrounding of palatal mesenchymal condensation and then invaded the condensation in a sprouting fashion. At the transcriptome level, we found 78 differentially expressed genes related to osteogenesis and angiogenesis between the ppmx and ppp. Fifty-five related genes were up/downregulated from E14.5 to E16.5. Here, we described the morphogenesis and the heterogeneity in the osteogenic and angiogenic genes profiles of the ppmx and ppp, which are significant for subsequent studies of normal and abnormal subjects.

KEYWORDS

angiogenesis, heterogeneity, osteogenesis, ppmx, ppp

1 | INTRODUCTION

Structurally, the palate is divided into the anterior bony hard palate and the posterior soft palate. Based on embryological origins, the palate comprises primary and secondary palates (Li et al., 2017). The primary palate extends from the premaxillary bone to the incisive foramen. The secondary palate consists of the remaining hard palate and the muscular soft palate. The secondary palate-derived

hard palate comprises the palatal process of the maxilla (ppmx) and the palatal process of the palatine (ppp) (Xu et al., 2018) and separates the oral cavity from the nasal cavity, ensuring normal swallowing, speech, and hearing (Boyce et al., 2018). The hard palate represents an attractive target for tissue regeneration engineering, which requires an accurate understanding of morphogenesis and the molecular mechanism of palatal osteogenesis. Studies on palatal osteogenesis, however, are quite few and limited (Bush & Jiang, 2012).

Osteogenesis is a complicated process, but only early osteoblast differentiation is discussed in current studies (Baek et al., 2011; Pauws et al., 2009; Wang et al., 2020; Xu et al., 2018, 2019). In addition, the investigated periods of early osteoblast differentiation differ in multiple publications, making it difficult to understand hard palate development.

It is known that the hard palate forms through intramembranous ossification (Percival & Richtsmeier, 2013; Santagati & Rijli, 2003), but no publication has described the normal osteogenesis process of the hard palate thus far. Intramembranous ossification includes the pre-osteogenic stage and post-condensation stage (Veselá et al., 2019). In the pre-osteogenic phase, mesenchymal cells condense; this occurrence has been shown in several studies (Baek et al., 2011; Goodwin et al., 2020; Li et al., 2021; Wang et al., 2020). In the post-condensation period, osteogenesis and angiogenesis dominate (Grosso et al., 2017), covering bone cells differentiation, extracellular matrix (ECM) assembly and mineralization, and vascularization. Osteogenesis is controlled by multiple genes. Runx2 governs the osteogenic fate of multipotent mesenchymal stromal cells (Pratap et al., 2003). *Osx*, downstream of Runx2, is involved in the full differentiation of osteoblasts (Nakashima et al., 2002). Preosteoblasts undergo three well-characterized differentiation stages to become mature osteoblasts (Rutkovskiy et al., 2016; Stein et al., 2004). First-stage osteoblasts predominantly proliferate and express *Fn*, collagens, and *Opn*. In the second stage, osteoblasts exit the cell cycle and start differentiation, which is accompanied by the expression of alkaline phosphatase and collagen as well as the maturation of bone ECM. In the third stage, osteoblasts mature and secrete abundant *Ocn* (Rutkovskiy et al., 2016). Although some aspects of expression have been published in the context of comparison to mutant models (Baek et al., 2011; Levi et al., 2011; Wang et al., 2020; Xu et al., 2018, 2019), single studies presenting the dynamic expression of osteogenic genes during hard palate development are lacking. Much has been written on osteoclasts, but no reports have been published about osteoclast biology in the hard palate. Osteoclasts are of hematopoietic origin (Burger et al., 1982) and proceed through a series of differentiation stages to produce multinucleated bone-resorbing cells. Osteoclast lineages specifically express tartrate-resistant acid phosphatase (TRAP) (M S Burstone, 1959). Pertinently, osteogenesis is tightly coupled with angiogenesis. Endochondral angiogenesis has been the subject of most studies, but intramembranous angiogenesis is poorly understood (Percival & Richtsmeier, 2013), especially angiogenesis of the hard palate. Angiogenesis refers to endothelial cells differentiating to form new blood vessels, and CD31 is commonly used as a marker of endothelial cells (Rakocevic et al., 2017). Therefore, the expression profile of these molecular markers in the hard palate can be used to outline the process by which palatal mesenchymal condensation develops into a mineralized bone structure.

Osteogenesis and angiogenesis are controlled by multiple signaling pathways. Genes expression patterns present site-specific heterogeneity along the anteroposterior axis of the secondary palate (Baek et al., 2011; Li et al., 2017; Liu et al., 2008; Pauws et al., 2009; Smith et al., 2012; Welsh & O'Brien, 2009; Xu et al., 2019; Yu et al.,

2005; Zhang et al., 2002). Notably, *Msx1* (Zhang et al., 2002) and *Shox2* (Xu et al., 2019; Yu et al., 2005) are specifically expressed in the anterior secondary palate, whereas the expression of *Meox2* and *Tbx22* is restricted to the posterior palate. *Bmpr1a* has preferential expression in the anterior secondary palate (Baek et al., 2011). Also, *Barx1* and *Mn1* have a posterior-predominant expression profile within the developing secondary palate (Liu et al., 2008; Welsh & O'Brien, 2009). Different gene expression patterns along the anterior-posterior axis of the secondary palate indicate distinct developmental mechanisms, but the known mechanisms are still far from clear and warrant further investigation.

Therefore, the objective of this study was to elucidate the morphogenesis process of the hard palate and identify molecular signaling associated with osteogenesis and angiogenesis.

2 | METHODS

This study was approved by the Biomedical Ethics Committee of Fujian Medical University (FJMU IACUC 2020-0026).

2.1 | Micro-computed tomography analysis

Heads of embryos at embryonic day (E) 18.5 and adult mice were fixed in 4% paraformaldehyde and then transferred to 70% ethanol. A micro-computed tomography (micro-CT) system (Research Center of Stomatology, Guangzhou Medical University, Guangzhou, China) was used to scan tissue at a 12 mm thickness with 55 kV energy and 145 mA intensity (ICT40).

2.2 | Histology staining

Skinned heads of mice at E14.5 to E18.5 were fixed in 100% ethanol for 1 week, and then the calvaria and mandible were removed before tissues were infiltrated in 2% potassium hydroxide (KOH) solution for 4 h. Subsequently, tissues were incubated in Alizarin Red solution (1% KOH, 75 $\mu\text{g}\cdot\text{mL}^{-1}$ Alizarin Red-S [Sigma]) overnight. Tissues were then rinsed in 2% KOH solution for 1 h and finally stored in a mixture of 2% KOH and glycerine (1:1).

A TRAP kit (387A-1KT, Sigma, USA) and von Kossa kit (G3282, Solarbio, China) were used in this study.

2.3 | Immunofluorescence staining

Primary antibodies were used as follows: Runx2 (ab192256, Abcam, 1:300), *Osx* (ab22552, Abcam, 1:300), Col1 (ab34710, Abcam, 1:1000), *Opn* (ab218237, Abcam, 1:500), *Ocn* (ab93876, Abcam, 1:500), and CD31 (ab28364, Abcam, 1:300). The secondary antibodies Alexa Fluor 488 and Alexa Fluor 594 were used at a dilution of 1:250.

2.4 | Tissue separation

Timed pregnant mice were killed and soaked in 100% alcohol for one minute. Afterward, embryos were obtained and transferred to ice-cold Hanks liquid. The mandibles and skulls of the embryos were removed. The ppmx and ppp of E14.5 to E16.5 embryos ($n = 3$ for each group) were dissected out under a stereomicroscope (Supplementary material 1) and then stored in RNAlater (BI, Israel) for RNA sequencing (RNA-seq). We compared the expression patterns of osteogenic and angiogenic genes between the ppmx and ppp at E14.5, E15.5, and E16.5, with the ppmx groups were used as the control groups. We also analyzed changes in genes expression from E14.5 to E16.5. And there were E15.5 vs E14.5 pairwise and E16.5 vs E15.5 pairwise, with the E14.5 group and E15.5 group were used as the control groups, respectively.

3 | RESULTS

3.1 | Osteogenic and angiogenic evaluation of the ppmx and ppp

Palatal mesenchymal cells start to condense at E14.5 (Baek et al., 2011; Goodwin et al., 2020; Li et al., 2021), and a hard palate develops at approximately E18.5. Therefore, we overviewed the osteogenesis and angiogenesis process of the hard palate by elucidating the expression patterns of corresponding markers from E14.5 to E18.5.

At E14.5, mesenchymal precursors of the ppp were strongly positive for Runx2 and Col1 (Figure 1D, a, a'), moderately positive for Osx and Opn (Figure 1D, a", a'''), but negative for Ocn (Figure 1D, a'''). CD31-positive cells were mainly located in the loose mesenchyme surrounding mesenchymal condensation and started to invade the primordium (Figure 2K). Also, progenitor cells of posterior ppmx (ppmx-p) were slightly positive for Runx2 and Col1 (Figure 1C, a, a') but negative for Osx, Opn, and Ocn (Figure 1C, a", a'', a'''). CD31-positive cells were few and scattered in the surrounding loose mesenchyme (Figure 2F). No markers were detected in the anterior ppmx (ppmx-a) primordium (data not shown).

At E15.5, the ppp calcified first (Figure 1A, b'''). In the ppp, the expression of Osx and Ocn increased (Figure 1D, b'', b'''). Runx2, Col1, and Opn expression decreased (Figure 1D, b, b', b''). Abundant CD31-positive cells invaded the ppp primordium (Figure 2L). In the ppmx-p, Runx2 and Col1 were strongly expressed (Figure 1C, b, b'). The expression of Osx was evident, while the expression of Opn was rare, and no Ocn was detected (Figure 1C, b'', b''', b'''). A large number of CD31-positive cells were located around the mesenchymal condensation of the ppmx-p and started to invade the condensation (Figure 2G). Runx2 and Col1 (Figure 1B, a, a') were slightly expressed in the mesenchymal progenitors of the ppmx-a, and no other markers were detected.

At E16.5, the ppp extended toward the midline (Figure 1A, c'', c'''). The ppmx-p (Figure 1A, c', c''') and ppmx-a (Figure 1A, c''') were

ossified. In the ppp, Osx, and Ocn were strongly expressed (Figure 1D, c'', c'''). The expression of Runx2 and Opn was decreased (Figure 1D, c, c'''). Abundant blood vessels were detected (Figure 2M). To illustrate bone remodeling in the hard palate, we conducted TRAP staining of serial sections of the hard palate. The first small mononuclear TRAP-positive cells were detected in the ppp at E16.5 (Figure 3A). In the ppmx-p, Osx and Ocn were strongly expressed (Figure 1C, c'', c'''). The expression of Opn increased (Figure 1C, c'''), while the expression of Runx2 and Col1 was decreased (Figure 1C, c, c'). CD31-positive cells invaded the ppmx-p (Figure 2H). In the ppmx-a, Runx2 was visibly expressed, accompanied by rich synthesis of Col1 (Figure 1B, b, b'). In contrast, Osx and Opn were rarely expressed (Figure 1B, b'', b'''). CD31-positive cells were adjacent to the mesenchymal condensation of the ppmx-a (Figure 2C).

At E17.5, the bilateral ppps approached each other (Figure 1A, d'', d'''), and the ppmx extended toward the primary palate (Figure 1A, d, d'''). The expression of osteogenic markers was decreased in the ppp and ppmx-p (data not shown), and blood vessels had been formed (Figure 2I,N). The first TRAP-positive cells in the ppmx-p were detected (Figure 3B). In the ppmx-a, the expression of Runx2 and Col1 was reduced (Figure 1B, c, c'). The expression of Osx, Opn, and Ocn was significantly increased (Figure 1B, c'', c''', c'''). Sprouting blood vessels invaded the mesenchymal condensation of the ppmx-a (Figure 2D).

By E18.5, a blood vessel-rich bone structure had been formed in the hard palate (Figure 2E,J,O). Also, bone remodeling had started. Many TRAP-positive cells were scattered in the ppp (Figure 3F). Most osteoclasts are typically elliptical, with one side facing the bone and the other side adjacent to the blood vessels (Cappariello et al., 2014). Compared with the oral side, osteoclasts exclusively lined on the bone surface of the nasal side of the ppp. In the ppmx, there was a single giant osteoclast lining, which had numerous nuclei, on the bone surface of the lateral-nasal side of the ppmx (Figure 3D,E).

Our data demonstrated that the active period in which the hard palate ossified and vascularized corresponded to E14.5 to E16.5.

3.2 | Expression patterns of osteogenic and angiogenic genes in the hard palate

To elucidate the heterogeneity of the molecular mechanisms of palatal osteogenesis along the anteroposterior axis of the secondary palate, the ppmx and ppp at E14.5 to E16.5 were collected for RNA-Seq. We found that the ppmx and ppp presented obvious transcriptome differences. Gene Ontology (GO) annotation of the differentially expressed genes (DEGs) showed that in the top 10 enrichment scores of biological processes, most terms of E14.5 were related to muscle development, while terms at E16.5 were mainly related to the nervous system (Figure 4). Bone-associated terms were detected at E15.5 (Figure 4). Therefore, RNAs with fragments per kilobase of transcript per million mapped reads (fpkm) ≥ 1 at E15.5 were subjected to GO analysis, and the results were summarized according to the biological processes covering bone formation, osteoblasts,

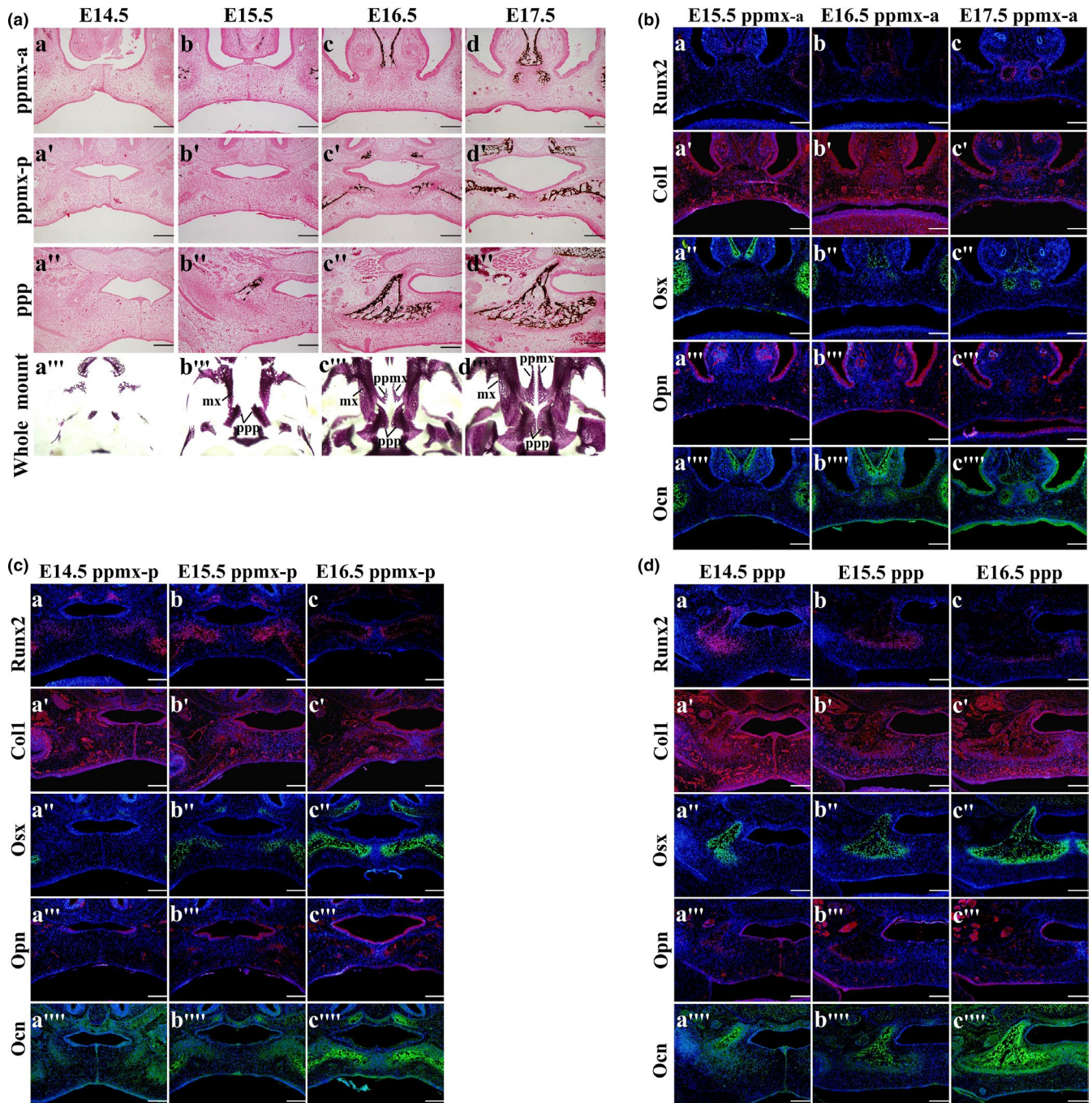


FIGURE 1 Osteogenesis process of the hard palate. (a) Morphogenesis of the hard palate from E14.5 to E17.5. a–d, a'–d' and a''–d'', von Kossa staining, morphogenesis of the hard palate in the coronal view. a'''–d''', Alizarin red staining, morphogenesis of the hard palate in the transverse view. mx, maxilla; ppmx, palatal process of the maxilla; ppp, palatal process of the palatine. (b–d) Immunofluorescence staining, expression patterns of Runx2, Col1, Osx, Opn, and Ocn during palatal osteogenesis. B, ppmx-a; C, ppmx-p; D, ppp. Scale bar = 502 μ m

blood vessels, and osteoclasts (Supplementary material 2–5). The expression of these genes between the ppmx and ppp was then followed by statistical analysis. Through filtering based on fold change (FC) ≥ 2 and false discovery rate (FDR) (adjusted p -value) < 0.05 , 78 DEGs between the ppmx and ppp were obtained at E15.5 (Table 1). Most DEGs at E14.5 and E16.5 were the same with the E15.5 group (Supplementary material 6–7). Through $|\log_2FC| \geq 2$ filtering, the

most striking DEGs in the ppp at E15.5 were Scn10a, Col9a1, Myog, Tnnt2, Col2a1, Col11a2, Spp1/Opn, Dmp1, Thbs4, Myl3, Adcyap1, Ibsp, Tac1, Rflna, Cacna1b, Foxc2, Kazald1, Npy1r, Cthrc1, Scg2, Col11a1, Ramp1, and Scx, and the most striking DEGs in ppmx were Mir23b, Shox2, Wnt5a, Alx1, and Dnm3os.

During osteogenesis, a series of successive and overlapping events occurred, which were regulated by specific genes. Therefore, we

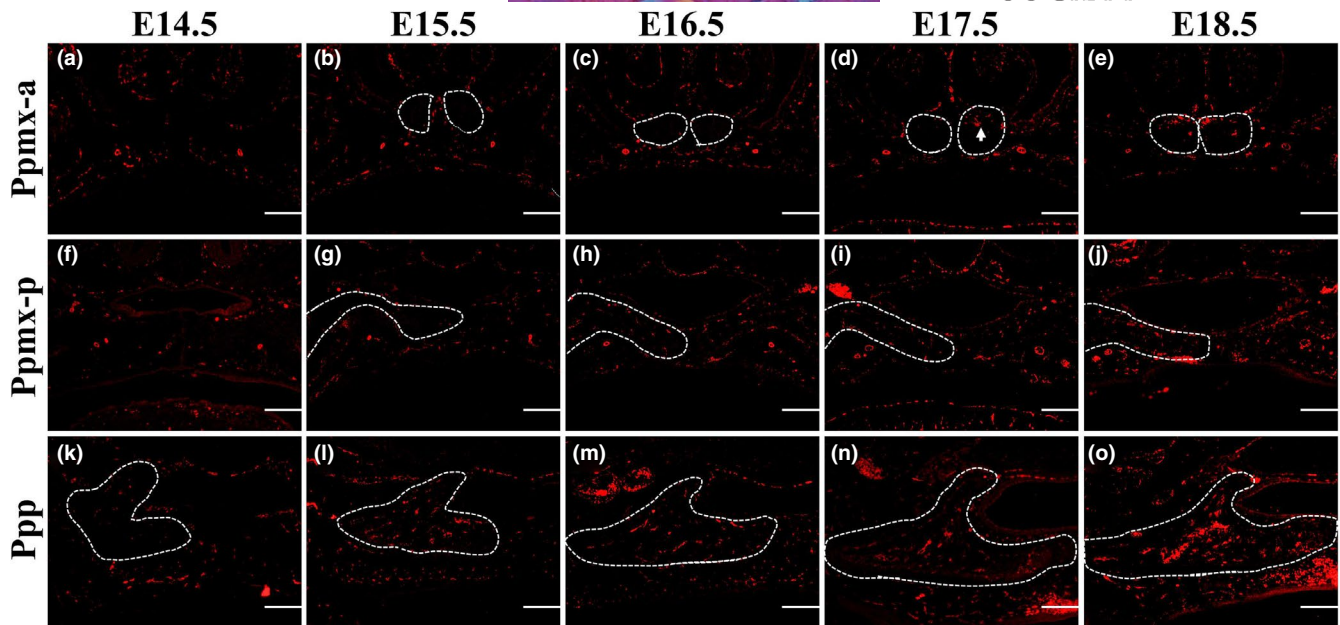


FIGURE 2 Angiogenesis process of the hard palate. (a–o) Immunofluorescence staining, expression patterns of CD-31 in the ppmx and ppp from E14.5 to E18.5. White dotted line, palatal processes; arrow, sprouting angiogenesis. Scale bar = 502 μ m

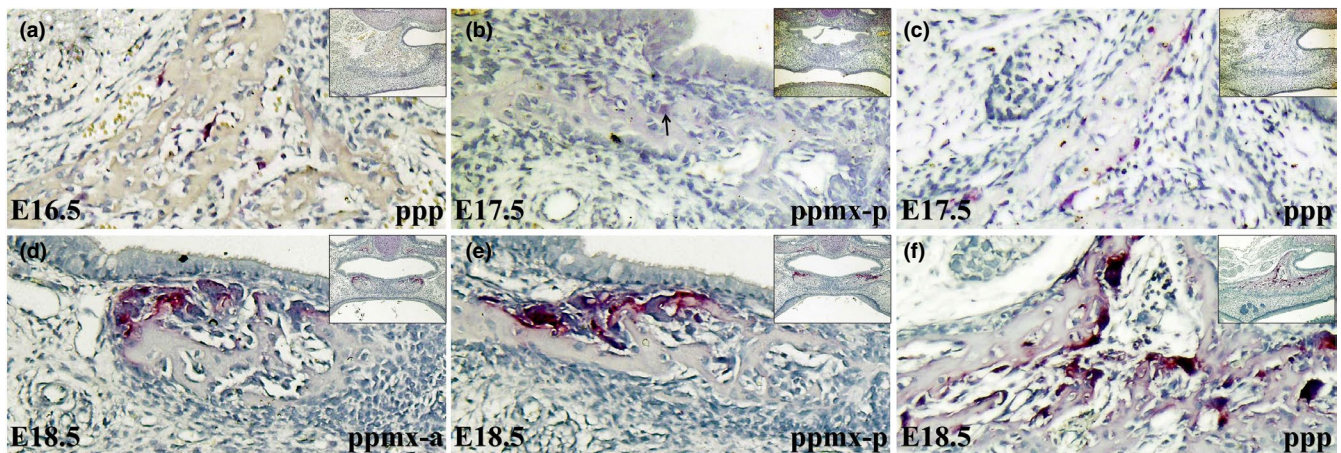


FIGURE 3 Osteoclastogenesis in the hard palate. (a–f) TRAP staining, osteoclast lineage in the ppmx and ppp from E16.5 to E18.5. The small image in the upper right corner of each picture shows the distribution of osteoclasts on the lateral-medial and nasal-oral sides of the hard palate. Arrow, TRAP-positive cell. Scale bar = 502 μ m

compared gene expression from E14.5 to E16.5 (E15.5 vs E14.5 and E16.5 vs E15.5). Through $FC \geq 2$ and $FDR < 0.05$ filtering, 55 genes were found to be significantly up/downregulated in the hard palate (Table 2). Through $|\log_2 FC| \geq 2$ filtering, genes with the most striking expression alterations were *Ltf*, *Dmp1*, *Spp1*, *Ibsp*, *Col11a2*, *Ifitm5*, *Ramp1*, and *Kazald1* in the ppmx and *Foxn4*, *Ltf*, *Cma1*, *Myl3*, and *Spp1* in the ppp.

Finally, through GO annotation, we revealed the possible specific roles of the osteogenic and angiogenic genes during hard palate development in Tables 3–4. Thus, we have outlined the molecular network associated with osteogenesis and angiogenesis in the ppmx and ppp.

4 | DISCUSSION

The maxillofacial region performs critical roles in daily life. Some maxillofacial tissues, including teeth (Catón & Tucker, 2009; Zhang et al., 2005), jaws (Parada & Chai, 2015; Suzuki et al., 2016; Svandova et al., 2020; Yuan & Chai, 2019), tongue (Parada et al., 2012), and lips (Jiang et al., 2006), have been extensively studied. Basic studies on the hard palate, however, are scarce (Baek et al., 2011; Bush & Jiang, 2012; Pauws et al., 2009; Wang et al., 2020; Xu et al., 2018, 2019). The present study is the first on the normal osteogenesis and angiogenesis of the hard palate.

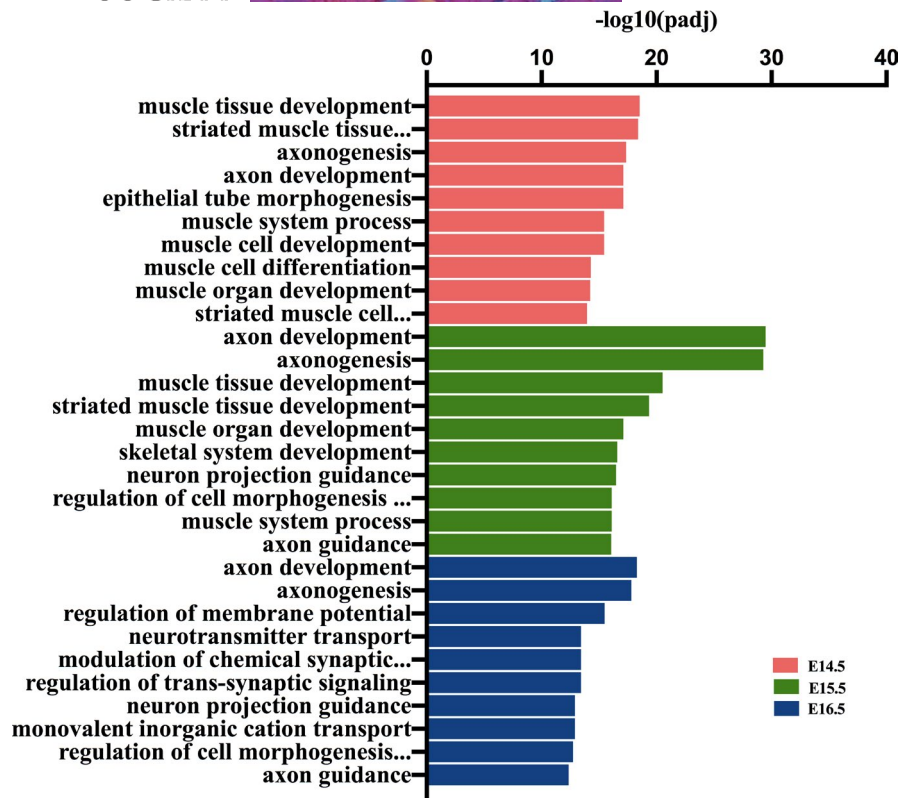


FIGURE 4 GO annotation of the DEGs between the ppmx and ppp at E14.5 to E16.5, with the top 10 enrichment scores, in terms of biological process

Bone defects of the hard palate are known as submucous cleft palate (SMCP) (Calnan, 1954), a subtype of cleft palate (Burg et al., 2016), with a reported incidence of 1:1250 to 1:5000 (Velasco et al., 1988; Weatherley-White et al., 1972). Knowledge of the physiology of the hard palate is indispensable for the etiology studies of SMCP (Clarke, 2008). In recent phenotypic studies, Runx2 was always used to assess osteoblast differentiation (Baek et al., 2011; Pauws et al., 2009; Wang et al., 2020; Xu et al., 2019), but the presence of Runx2 alone is not enough to sustain complete osteoblast differentiation (Komori, 2010), as osteoblasts still need to go through three distinct differentiation stages (Rutkovskiy et al., 2016). The expression patterns of markers of each stage demonstrate that the main period of osteoblast differentiation and maturation in the hard palate corresponds to E14.5 to E16.5. And the results of expression patterns of osteogenic genes can be used to assess the palatal osteogenesis in the subsequent abnormal studies. Osteoclasts are responsible for bone resorption (Cappariello et al., 2014). In line with the notion of bone site-specific osteoclast heterogeneity (Falconi et al., 2011; Everts et al., 2009; Goldberg et al., 2016; Perez-Amodio et al., 2006; Quarto et al., 2010), we found for the first time that osteoclasts of the ppmx and ppp showed obvious differences in cell and nuclei number, size, morphology, and distribution. We assume that asymmetric bone remodeling in the hard palate is due to the expansion of the nasal cavity. Osteoclast heterogeneity implies differences in local bone remodeling and corresponding treatment strategies (Everts et al., 2009). Therefore, more studies are called to provide

further insights into the detailed characteristics of the morphology and functions of osteoclasts in the ppmx and ppp. Pertinently, osteogenesis is tightly coupled with angiogenesis (Cappariello et al., 2014). Here, we provide the first insight into the angiogenesis of the hard palate. In contrast to mouse limb buds (Eshkar-Oren et al., 2009), an avascular layer of loose mesenchyme was not observed during vascularization of the hard palate, indicating distinct developmental mechanisms between endochondral angiogenesis and intramembranous angiogenesis. Intussusceptive angiogenesis, in which the primary blood vessel splits into two vessels through the transcapillary tissue pillar without endothelial cell proliferation, was detected during craniofacial bone development (Spiegelaere et al., 2010). However, our histological data showed capillaries in the surrounding loose mesenchyme sprouts and invaded the palatal mesenchymal condensation, suggesting sprouting angiogenesis (Maes et al., 2010) in the hard palate. This finding is further supported by the substantial number of genes associated with sprouting angiogenesis shown in Table 4. Although osteogenesis is closely accompanied by angiogenesis, whether variation in angiogenesis causes bone defects is still unknown (Brandi & Collin-Osdoby, 2006), and should be investigated in further studies.

Distinct gene patterns between the ppmx and ppp have been demonstrated (Pauws et al., 2009; Xu et al., 2019). Our RNA-seq analysis provided a comprehensive understanding of the molecular heterogeneity between the ppmx and ppp. Consistent with previous works, Shox2 (Xu et al., 2019) had a higher expression in the

TABLE 1 DEGs associated with osteogenesis and angiogenesis between the ppmx and ppp at E15.5. $|\log_2FC| \geq 1$ and $-\log_{10}(padj) > 1.30103$ were used as the thresholds

Symbol	\log_2FC	Padj	Symbol	\log_2FC	Padj
High expression in the ppp					
Scn10a	9.591499538	2.49E-12	Ifitm5	1.851754718	3.83E-13
Col9a1	6.570633904	1.96E-67	Papss2	1.837963094	5.43E-52
Myog	6.303915197	2.28E-114	Ank2	1.829135049	2.51E-42
Tnnt2	5.898981913	4.77E-93	Mgp	1.742981717	2.18E-41
Col2a1	5.744304477	0	Ehd3	1.643032172	2.23E-15
Col11a2	5.704230139	0	Isl1	1.638112603	0.027915933
Spp1	5.148137557	4.10E-247	Bmper	1.581241277	6.25E-21
Dmp1	4.991634104	1.57E-79	Akap6	1.446914446	3.78E-10
Thbs4	4.217114168	1.78E-108	Col27a1	1.439996102	1.21E-29
Myl3	4.146011115	1.17E-18	Nov	1.42649332	8.68E-22
Adcyap1	4.003542866	2.48E-15	Foxc1	1.39633194	3.59E-24
Ibsp	3.809411598	1.44E-23	Fzd9	1.38497715	7.00E-16
Tac1	3.578181803	6.07E-20	Fam20c	1.350633496	2.13E-17
Rflna	3.316821695	3.66E-37	Sema3c	1.339160102	3.51E-29
Cacna1b	3.310130619	2.48E-38	Cspg4	1.263057425	5.35E-22
Foxc2	3.004089488	4.08E-53	Sparc	1.210904981	2.57E-19
Kazald1	2.699804254	3.90E-56	Mmp9	1.202183164	5.28E-10
Npy1r	2.621082966	1.08E-12	Fgfr3	1.197479491	1.43E-18
Cthrc1	2.55430716	2.67E-115	Dlx3	1.114111316	5.02E-08
Scg2	2.48744079	1.01E-20	Gpm6b	1.105363816	2.59E-22
Col11a1	2.333644302	3.55E-103	Fap	1.061569852	2.02E-15
Ramp1	2.159554058	1.52E-29	Ctsk	1.031890629	7.04E-18
Scx	2.089468826	1.23E-30	Kcna5	1.031170175	2.08E-05
Aldh1a2	1.944167101	2.89E-50	Rspo3	1.02591278	3.76E-09
Meox2	1.914361189	1.45E-28	Penk	1.012068873	2.25E-15
High expression in the ppmx					
Mir23b	-5.018114542	0.000232574	F2rl1	-1.194842949	1.52E-08
Shox2	-3.199056015	1.87E-201	Osr2	-1.192260465	5.70E-21
Wnt5a	-2.465423799	2.62E-60	Wnt4	-1.189283116	5.08E-25
Alx1	-2.23040588	2.52E-08	Meis1	-1.185517387	3.97E-18
Dnm3os	-2.028866374	4.16E-48	Ednra	-1.1643281	1.66E-14
Dsg2	-1.957744884	9.07E-43	Frem1	-1.152077166	1.11E-18
Cyp26b1	-1.828771248	1.58E-64	Lrp5	-1.122373497	3.07E-17
Cma1	-1.809241542	2.21E-07	F3	-1.122091691	5.48E-12
Spint1	-1.644091561	4.36E-26	Arid5b	-1.115445376	8.75E-12
Foxn4	-1.466455897	6.94E-11	Plxnb1	-1.088087234	7.93E-32
Epha1	-1.348374277	1.15E-18	Cacna1c	-1.046899968	1.19E-15
Tnc	-1.308829953	9.96E-26	Mmp13	-1.035840382	0.000124128
Prrx1	-1.289753145	2.73E-36	Alx4	-1.012359884	1.84E-15
Foxf2	-1.271639053	6.64E-12	Sfrp2	-1.007554322	1.89E-19

ppmx, and Meox2 (Baek et al., 2011) had a higher expression in the ppp. However, no difference was detected in the expression of Msx1 (Zhang et al., 2002), Bmpr1a (Baek et al., 2011) and Tbx22 (Pauws et al., 2009) between the ppm and ppp. Also, according to Pauws

et al (Pauws et al., 2009), Tbx22 expression was restricted to the posterior secondary palate at E13.5, while we found that Tbx22 expression showed no difference between the ppm and ppp during E14.5 to E16.5. Bmpr1a is reported to have anterior-predominant

TABLE 2 Alterations in the expression of genes associated with osteogenesis and angiogenesis in the hard palate from E14.5 to E16.5.

Symbol	log ₂ FC	Padj	Symbol	log ₂ FC	Padj
Up/downregulated genes in the ppmx					
E15.5 vs E14.5					
Ltf*	2.15378898	0.043021091	Ctsh	1.237571711	5.64E-10
Foxn4	1.557394999	2.69E-07	Tyrobp	1.044075577	4.78E-05
Lgals3*	1.437719272	8.06E-12	Hspb1*	1.036045595	1.65E-08
Cma1*	1.36656634	4.44E-05	F2rl1	1.031570169	5.63E-06
Omd	1.334254895	0.032271601	Mmp9	-1.45320693	8.80E-25
Agt*	1.268471791	0.000317523			
E16.5 vs E15.5					
Dmp1	4.893081456	9.68E-18	Apoe	1.384113672	1.44E-27
Spp1	4.357012202	3.23E-23	Cma1*	1.350053063	4.40E-08
lbsp	3.999788019	2.14E-40	Col1a1	1.303618956	1.56E-19
Ltf*	3.527561242	3.55E-60	Tmem119	1.284455644	2.40E-27
Col11a2	3.226632731	1.01E-97	Sparc	1.254426106	5.69E-24
lfitm5	2.667139769	1.25E-52	Junb	1.219990382	1.46E-12
Ramp1	2.496575838	1.43E-37	Sp7	1.112163014	2.50E-10
Kazald1	2.333194143	7.35E-30	Ctsk	1.090241856	5.93E-20
Thbs4	1.844485995	4.16E-09	Penk	1.08660747	6.51E-18
Lgals3*	1.708034468	1.17E-23	Col1a2	1.062894677	7.00E-13
Agt*	1.558723803	5.72E-17	lfitm1	1.022842904	4.56E-08
Hspb1*	1.515062516	3.33E-19	Cebpb	1.00611054	4.57E-10
Dlx3	1.513046123	2.24E-22	Vkorc1	1.003499791	0.000321281
Mgp	1.454681049	2.67E-32	Sox11	-1.001192676	6.97E-10
Cd36	1.429263433	1.23E-10	Shox2	-1.03305727	1.11E-20
Cthrc1	1.429221534	2.22E-19	Asb4	-1.414681717	5.62E-18
Up/downregulated genes in the ppp					
E15.5 vs E14.5					
Foxn4	3.660115444	7.28E-13	Thy1	1.227010303	9.04E-05
Ltf*	3.479635311	8.54E-12	Col11a1	1.14810264	0.025309416
Cma1*	2.310002924	0.000108205	Klf5	1.117954649	5.61E-05
Myl3	2.158833966	1.39E-08	Hspb1	1.115826523	5.41E-09
Spp1	2.000435645	0.005462396	Wnt7b	1.113565905	9.92E-07
Agt	1.75550345	1.76E-07	Ctsh	1.113400904	5.23E-11
Nov	1.545673867	7.74E-18	Pf4	1.072620078	0.000520339
Dmp1	1.43026483	0.049514675	Dnm3os	-1.607919034	4.82E-15
Lgals3	1.326787269	0.000318359			
E16.5 vs E15.5					
Cma1*	1.561561868	0.044229736	Ltf*	1.662509957	1.11E-05

Note: Genes detected in both the E15.5 vs E14.5 group and E16.5 vs E15.5 group are marked with an asterisk.

expression in the secondary palate (Baek et al., 2011), but we agree that there is no difference in the expression of Bmpr1a between the ppmx and ppp. This expression pattern can account for the bone defect in both the ppmx and ppp of Bmpr1a-deficient embryos (Baek et al., 2011). Barx (Welsh & O'Brien, 2009) and Mn1 (Liu et al., 2008) have posterior-predominant expression in the secondary palate. We found that Barx1 expression was higher in the ppp, but

the expression of Mn1 was higher in the ppmx, and neither of these levels of expression was statistically significant. Mn1 acts upstream of Tbx22 (Liu et al., 2008), and neither differed in expression between the ppmx and ppp during the investigated period. Therefore, more research is needed to understand the dynamic expression and function of Mn1 and Tbx22 in the hard palate. Notably, Wnt5a, Osr2, and Mir23b in the palate (Ding et al., 2016; Li, et al., 2017)

TABLE 3 Schematic of the hard palate progression in the context of osteogenic genes detected by RNA-seq at E15.5

Osteoblast fate commitment	Smad5	Dlx5	Sh3pxd2b	Smad1	Runx2	Men1	Gli	
<i>Sp7</i>								
Osteoblast proliferation	<i>Lrp5</i>	<i>Sfrp1</i>	<i>Tmem119</i>	<i>Cthrc1</i>	<i>Abl1</i>	<i>Atraid</i>	<i>Cyr61</i>	<i>Lrrc17</i>
<i>Osr2</i>								<i>Sfrp1</i>
Rhoa								
Osteoblast differentiation	<i>Tnc</i>	<i>Satb2</i>	<i>Wnt4</i>	<i>Axin2</i>	<i>Vegfa</i>	<i>Bmp2</i>	<i>Fbn2</i>	<i>Id4</i>
<i>Lrp5*</i>	<i>Igf1</i>	<i>Npnt</i>	<i>Igfbp3</i>	<i>Penk</i>	<i>Penk</i>	<i>Mmp13</i>	<i>Col1a1</i>	<i>Tmem119</i>
<i>Cebpb</i>	<i>Sp7</i>	<i>Sox11</i>	<i>Cthrc1</i>	<i>Spp1</i>	<i>Spp1</i>	<i>Shox2</i>	<i>Ski*</i>	<i>Sox2*</i>
<i>Fgfr1*</i>	<i>Tmem64*</i>	<i>Id2*</i>	<i>Nbr1*</i>	<i>Igfbp5*</i>	<i>Igfbp5*</i>	<i>Sfrp1*</i>	<i>Men1*</i>	<i>Vcan</i>
<i>Iars</i>	<i>Smo</i>	<i>Col6a1</i>	<i>Cat</i>	<i>Erh</i>	<i>Erh</i>	<i>Twsg1*</i>	<i>Ddr2</i>	<i>Psmc2</i>
<i>Dhx9</i>	<i>Atp6ap1</i>	<i>Lrrc17</i>	<i>Rps11</i>	<i>Clic1</i>	<i>Clic1</i>	<i>Snmnp200</i>	<i>Rack1</i>	<i>Rrbp1</i>
<i>Atp5b</i>	<i>Lmna</i>	<i>Hnrnpu</i>	<i>Pth1R</i>	<i>Cd276</i>	<i>Cd276</i>	<i>Hsd17b4</i>	<i>Tgfb3</i>	<i>Wwtr1</i>
<i>H3f3b</i>	<i>H3f3a</i>	<i>Igf2</i>	<i>Snd1</i>	<i>Rras2</i>	<i>Rras2</i>	<i>Hspe1</i>	<i>Cyr61</i>	<i>Trp53lnp2</i>
<i>Rsl1d1</i>	<i>Mybbp1a</i>	<i>Fasn</i>	<i>Syncrip</i>	<i>Id1</i>	<i>Id1</i>	<i>Wnt11</i>	<i>Akt1</i>	<i>Mef2d</i>
<i>Snai2</i>	<i>Alpl</i>	<i>Hnrnpc</i>	<i>Tmsb4x</i>	<i>RbmX</i>	<i>RbmX</i>	<i>Lgr4</i>	<i>Rdh14</i>	<i>Ddx5</i>
<i>Hdac5</i>	<i>Cebpa</i>	<i>Gli1</i>	<i>Atraid</i>	<i>Dlx5</i>	<i>Dlx5</i>	<i>Rps15</i>	<i>Tob1</i>	<i>Hdac7</i>
<i>Pdlim7</i>	<i>Gja1</i>	<i>Esrra</i>	<i>Acvr1</i>	<i>Smad1</i>	<i>Smad1</i>	<i>Jag1</i>	<i>Ptch1</i>	<i>Nog</i>
<i>Fndc3b</i>	<i>Tpm4</i>	<i>Fbl</i>	<i>Bmp7</i>	<i>Pias2</i>	<i>Pias2</i>	<i>Mrc2</i>	<i>Bmp4</i>	<i>Creb3l1</i>
<i>Gli2</i>	<i>Ccdc47</i>	<i>Fhl2</i>						
ECM assembly								
<i>Gpm6b</i>	<i>Has2</i>	<i>Rgcc</i>	<i>Smad3</i>	<i>Tgfb1</i>	<i>Phldb1</i>	<i>Phldb2</i>	<i>Ramp2</i>	
Bone mineralization	<i>Fbn2</i>	<i>Osr2</i>	<i>Bmp6</i>	<i>Gpm6b</i>	<i>Wnt4</i>	<i>Twist1</i>	<i>Igf1</i>	<i>Tmem119</i>
<i>Mgp</i>	<i>Igf1m5</i>	<i>Gja1</i>	<i>Hif1a</i>	<i>Nbr1</i>	<i>Nbr1</i>	<i>Osr1</i>	<i>Sox9</i>	<i>Mia3</i>
<i>Ddr2</i>	<i>Bmpr1a</i>	<i>Atraid</i>	<i>Ptn</i>	<i>Pth1r</i>	<i>Pth1r</i>	<i>Rflnb</i>	<i>Gpc3</i>	<i>Fgfr2</i>
<i>Acvr1</i>	<i>Bmp4</i>	<i>Fzd9</i>	<i>Smad3</i>	<i>Tgfb1</i>	<i>Tgfb1</i>	<i>Ano6</i>	<i>Fgfr3</i>	<i>Pkdcc</i>
Bone trabeculae formation	<i>Fbn2</i>	<i>Vegfa</i>	<i>Col1a1</i>	<i>Mmp2</i>	<i>Sfrp1</i>			
Osteoclast differentiation	<i>Ltf*</i>	<i>Fbn1*</i>	<i>Sfrp1*</i>	<i>Ctnnb1*</i>	<i>Anxa2</i>	<i>Efna2</i>	<i>Pafah1b1</i>	<i>Tmem64</i>
								<i>Src</i>

Note: DEGs are indicated in red; up/downregulated genes are depicted in blue; genes with temporal and spatial differences in expression are shown in green; negative genes are marked by an asterisk.

TABLE 4 Schematic of the hard palate progression in the context of angiogenic genes detected by RNA-seq at E15.5

Blood vessel endothelial cell fate commitment									
Hey2	Nr2f2	Rbpj	Smo	Nrp1					
Patterns of blood vessels									
Lrp5	Vegfa	Ednra	Sfrp2	Tgfr2	Nfatc4	Srf	Ppp3r1	Cxcl12	Plxnd1
Col4a1	Ctnnb1	Bax	Eng						
Blood vessel endothelial cell proliferation									
Gata2	Bmp6r	Vegfa	Ngfr	Pdcd10	Acvr1l	Itgb1bp1	Sema5a	Hmox1	Bmp4
Epha2	Thbs1	Hmgb1	Fgfr1	Plcg1	Mef2c				
Blood vessel endothelial cell differentiation									
Hey2	Nr2f2	Nrp1	Tmem100	Notch1	Rbpj	Ccm2	Hey1	Notch3	Smo
Kdr									
Blood vessel endothelial cell migration									
Vegfa	Foxc2	Gata2	Slit2	Meox2*	Vash1*	Hspb1	Apoe*	Csnk2b*	Rgcc*
Pdcd10*	Rhoa*	Map2k*	Tgfb1*	Mef2c*	Tbxa21*	Mmrn2*	Itgb1bp*	Hmgb1*	Acvr1l*
Hdac5*	Thbs1*	Notch*	Klf4*	Id1*	Cdc42	Vhl	Mapk14	Reck	Srf
Amot1l	Cib1	Amot	Kdr	Nus1	Lemd3	Efnb2	Smo	Hmox1	Itga5
Plxnd1	Cdh5	Fgf18	Nfe2l2	Nrp1	Clec14a	Ephb4	Hspg2	Hdac7	Map3k3
Angpt1	Hif1a	Ets1	Robo1	Sirt1	Sox18	Akt1	Prkd2	Prkd1	Gpx1
Plcg1	Ecscr	Atp5b	Myh9	Vegfc	Nr4a1	Pdgfb	Fgfr1	Itgb1	Nos3
Prkca	P2rx4	Prcp							
Blood vessel branching									
Ednra	Foxc2	Vegfa	Sfrp2	Srf	Nrp1	Stk4	Gna13	Ppp3r1	Ctnnb1
Plxnd1	Nfatc4	Tgfr2	Col4a1	Eng	Acvr1	Kdr	Unc5b	Ahr	Pitx2
Nfatc3	Sema5a	Cxcr4	Vegfc	Vangl2	Tbx1	Cxcl12	Angpt1	Tek	
Blood vessel remodeling									
Sema3c	Foxc1	Abr*	Jag1	Pbrm1	Epas1	Ahr	Tgfr3	Mdm2	Tgfb2
Bak1	Erg	Atg5	Tgm2	S1pr1	Tgfb1	Gja1			
Blood circulation									
Npy1r	Cacna1b	Akap6	Adcyap1	Ehd3	Scn10a	Ank2	Hey2	Tac1	Dsg2
Per2	Cx3cl1	F2rl1	Myl3	Tnnt2	Foxn4	P2ry1	Kcnj2	Prkg1	Nos3
Nppc	Ptgs1	Tbxa2r	Prkca	Gja5	Kat2b	Adra1d	Kcna5	Cacna1c	P2rx4
Adora2b	Hdac4	Sp4	Gper1	Akap9	Slc8a1	Icam1	Pde5a	Ada	Hbegf
Scn2b									
Apoptotic process involved in blood vessel morphogenesis									
Lrp5	Wnt7b	Bak1	Spi1	Angptl4	Bax				

Note: DEGs are indicated in red; up/downregulated genes are depicted in blue; genes with temporal and spatial differences in expression are shown in green; negative regulators are marked by an asterisk.

had higher expression in the ppmx. The anterior secondary palate is thought to be more important because there are numerous specific genes (Smith et al., 2012), but we found 50 DGEs in the ppp and 28 DEGs in the ppmx. The collagens of the secondary palate (Logan et al., 2020), including Col2a1, Col9a1, Col11a1, Col11a2, and Col27a1, are mainly expressed in the ppp. Furthermore, annotation of DEGs in the ppp through the NCBI Gene Database showed that Spp1, Dmp1, Ibsp, Kazald1, Ifitm5, Mgp, Bmper, Fad9, Fam20c, Sparc, Mmp9, Fgfr3, Gpm6b, Ctsk, and Rspo3 have a role in osteogenesis and that Ctrc1 acts on angiogenesis. Retinoic acid regulates the expression of Spp1 in the palate (Peng et al., 2020), and Aldh1a2, which is highly expressed in the ppp, can promote the synthesis of retinoic acid (Shabtai et al., 2016), suggesting the possible role of Aldh1a2 in osteogenesis in the ppp. Regarding ppmx DEGs, Cy26b1, Wnt4, Lrp5, Mmp13, and Alx4 are critical for osteogenesis, and Cmal, F2r11, Ednral, and F3 are required for angiogenesis. Also, annotation of all the DEGs through the Kyoto Encyclopedia of Genes and Genomes (KEGG) database shows that Fzd9, Rspo3, Wnt4, Lrp5, F3, and Sfrp2 affect Wnt signaling, highlighting the significance of Wnt signaling during palatal osteogenesis. Therefore, more research is needed to explore the functions of these DEGs during hard palate development.

Hard palate ossifies in an intramembranous fashion (Percival, 2013; Santagati & Rijli, 2003), involving osteoblast differentiation, ECM assembly and mineralization, vascularization and osteoclast differentiation (Clarke, 2008; Matsuura et al., 2014). These events are controlled by specific molecules. Analysis of alterations in gene expression over time revealed that changes in gene expression in the ppp and ppmx mainly occurred at E15.5 and E16.5, respectively, which is consistent with the posterior-to-anterior osteogenesis pattern of the hard palate. The ppp was ossified in a very short period, and mesenchymal cells condensed at E14.5, ECM calcified at E15.5, and bone remodeling began at E16.5. Therefore, there were few osteogenic and angiogenic genes with altered expression in the ppp during the investigated period, with only the expression of the osteogenic gene Spp1 and angiogenic genes Foxn4, Myl3, Hspb1, and Wnt7b increasing during the investigated period, as shown in Tables 3-4. In the ppmx, as expected, genes involved in osteoblast differentiation, including Spp1, Ibsp, Cthrc1, Tmem119, Sp7, Penk, Ifitm1, and Cebpb, and genes functioning in bone mineralization, including Ifitm5, Tmem119, Ibsp, and Mgp, were increased at E16.5, as shown in Table 3. However, the expression of Sox11 and Shox2 was decreased, suggesting a function in early osteoblast differentiation (Xu et al., 2019). Paralleled the first osteoclasts detected in the ppmx at E17.5, Ctsk (Kiviranta et al., 2005) and Ltf were upregulated at E16.5. More research is needed to explore the specific roles of these genes during palatal osteogenesis. In addition, osteogenic and angiogenic genes with constant high expression or without expression differences between the ppmx and ppp warrant further investigation.

This study helps improve the present understanding of normal palatal osteogenesis, calls for more attention to be paid to hard palate development, and offers an essential foundation for subsequent studies of normal and abnormal subjects.

CONFLICT OF INTEREST

All the authors confirm that there are no conflicts of interest to disclose.

AUTHOR CONTRIBUTIONS

CYL designed the experiment; ML and YHH contributed to the data acquisition; CYL contributed to the data analysis and drafting of the manuscript; and CQM, CYR, and JPC revised the manuscript. MKL and WHC contributed to the critical revision of the manuscript and approved the article.

DATA AVAILABILITY STATEMENT

The data used to support the findings of this study are available from the corresponding author upon request.

ORCID

Weihui Chen  <https://orcid.org/0000-0001-6972-7695>

REFERENCES

- Baek, J.A., Lan, Y., Liu, H., Maltby, K.M., Mishina, Y. & Jiang, R. (2011) Bmpr1a signaling plays critical roles in palatal shelf growth and palatal bone formation. *Development Biology*, 350(2), 520–531. <https://doi.org/10.1016/j.ydbio.2010.12.028>
- Boyce, J.O., Kilpatrick, N. & Morgan, A.T. (2018) Speech and language characteristics in individuals with nonsyndromic submucous cleft palate—a systematic review. *Child Care Health Development*, 44(6), 818–831. <https://doi.org/10.1111/cch.12613>
- Brandi, M.L. & Collin-Osdoby, P. (2006) Vascular biology and the skeleton. *Journal of Bone and Mineral Research*, 21(2), 183–192. <https://doi.org/10.1359/JBMR.050917>
- Burg, M.L., Chai, Y., Yao, C.A., Magee, W. III & Figueiredo, J.C. (2016) Epidemiology, etiology, and treatment of isolated cleft palate. *Frontiers in Physiology*, 7, 67. <https://doi.org/10.3389/fphys.2016.00067>
- Burger, E.H., Meer, J.W.V.D., Gevel, J.S.V.D., Gribnau, J.C., Thesingh, G.W. & Furth, R.V. (1982) In vitro formation of osteoclasts from long-term cultures of bone marrow mononuclear phagocytes. *Journal of Experimental Medicine*, 156(6), 1604–1614. <https://doi.org/10.1084/jem.156.6.1604>
- Burstone, M.S. (1959) Histochemical demonstration of acid phosphatase activity in osteoclasts. *Journal of Histochemistry and Cytochemistry*, 7(1), 39–41.
- Bush, J.O. & Jiang, R. (2012) Palatogenesis: morphogenetic and molecular mechanisms of secondary palate development. *Development*, 139(2), 231–243. <https://doi.org/10.1242/dev.067082>
- Calnan, J. (1954) Submucous cleft palate. *Journal of Plastic Reconstructive and Aesthetic Surgery*, 6(4), 264–282.
- Cappariello, A., Maurizi, A., Veeriah, V. & Teti, A. (2014) The great beauty of the osteoclast. *Archives of Biochemistry and Biophysics*, 558, 70–78. <https://doi.org/10.1016/j.abb.2014.06.017>
- Catón, J. & Tucker, A.S. (2009) Current knowledge of tooth development: patterning and mineralization of the murine dentition. *Journal of Anatomy*, 214(4), 502–515. <https://doi.org/10.1111/j.1469-7580.2008.01014.x>
- Clarke, B. (2008) Normal bone anatomy and physiology. *Clinical Journal of the American Society of Nephrology*, 3(Supplement 3), S131–S139. <https://doi.org/10.2215/CJN.04151206>
- de Souza Faloni, A.P., Schoenmaker, T., Azari, A., Katchburian, E., Cerri, P.S., de Vries, T. J. et al. (2011) Jaw and long bone marrows have a different osteoclastogenic potential. *Calcified Tissue International*, 88(1), 63–74. <https://doi.org/10.1007/s00223-010-9418-4>

- Ding, H.-L., Hooper, J.E., Batzel, P., Eames, B.F., Postlethwait, J.H., Artinger, K.B. et al. (2016) MicroRNA profiling during craniofacial development: potential roles for Mir23b and Mir133b. *Frontiers in Physiology*, 7, 281. <https://doi.org/10.3389/fphys.2016.00281>
- Eshkar-Oren, I., Viukov, S.V., Salameh, S., Krief, S., Oh, C.-D., Akiyama, H. et al. (2009) The forming limb skeleton serves as a signaling center for limb vasculature patterning via regulation of Vegf. *Development*, 136(8), 1263–1272. <https://doi.org/10.1242/dev.034199>
- Everts, V., Vries, T.J.D. & Helfrich, M.H. (2009) Osteoclast heterogeneity: lessons from osteopetrosis and inflammatory conditions. *Biochimica Biophysica Acta*, 1792(8), 757–765. <https://doi.org/10.1016/j.bbdis.2009.05.004>
- Goldberg, S., Grynpas, M.D. & Glogauer, M. (2016) Heterogeneity of osteoclast activity and bone turnover in different skeletal sites. *Archives of Oral Biology*, 71, 134–143. <https://doi.org/10.1016/j.archoralbio.2016.06.026>
- Goodwin, A.F., Chen, C.P., Vo, N.T., Bush, J.O. & Klein, O.D. (2020) YAP/TAZ regulate elevation and bone formation of the mouse secondary palate. *Journal of Dental Research*, 99(12), 1387–1396. <https://doi.org/10.1177/0022034520935372>
- Grosso, A., Burger, M.G., Lunger, A., Schaefer, D.J., Banfi, A. & Maggio, N.D. (2017) It takes two to tango: coupling of angiogenesis and osteogenesis for bone regeneration. *Frontiers in Bioengineering and Biotechnology*, 5, 68. <https://doi.org/10.3389/fbioe.2017.00068>
- Jiang, R., Bush, J.O. & Lidral, A.C. (2006) Development of the upper lip: morphogenetic and molecular mechanisms. *Developmental Dynamics*, 235(5), 1152–1166. <https://doi.org/10.1002/dvdy.20646>
- Kiviranta, R., Morko, J., Alatalo, S.L., NicAmhlaibh, R., Risteli, J., Laitala-Leinonen, T. et al. (2005) Impaired bone resorption in cathepsin K-deficient mice is partially compensated for by enhanced osteoclastogenesis and increased expression of other proteases via an increased RANKL/OPG ratio. *Bone*, 36(1), 159–172. <https://doi.org/10.1016/j.bone.2004.09.020>
- Komori, T. (2010) Regulation of osteoblast differentiation by Runx2. *Advances in Experimental Medicine and Biology*, 658, 43–49.
- Levi, B., James, A.W., Nelson, E.R., Brugmann, S.A., Sorokin, M., Manu, A. et al. (2011) Role of Indian hedgehog signaling in palatal osteogenesis. *Plastic and Reconstructive Surgery*, 127(3), 1182–1190. <https://doi.org/10.1097/PRS.0b013e3182043a07>
- Li, C., Lan, Y. & Jiang, R. (2017) Molecular and cellular mechanisms of palate development. *Journal of Dental Research*, 96(11), 1184–1191. <https://doi.org/10.1177/0022034517703580>
- Li, N., Liu, J., Liu, H., Wang, S., Hu, P., Zhou, H. et al. (2021) Altered BMP-Smad4 signaling causes complete cleft palate by disturbing osteogenesis in palatal mesenchyme. *Journal of Molecular Histology*, 52(1), 45–61. <https://doi.org/10.1007/s10735-020-09922-4>
- Liu, W., Lan, Y., Pauws, E., Meester-Smoor, M.A., Stanier, P., Zwarthoff, E.C. et al. (2008) The Mn1 transcription factor acts upstream of Tbx22 and preferentially regulates posterior palate growth in mice. *Development*, 135(23), 3959–3968. <https://doi.org/10.1242/dev.025304>
- Logan, S.M., Ruest, L.B., Benson, M.D. & Svoboda, K.K.H. (2020) Extracellular matrix in secondary palate development. *Anatomical Record*, 303(6), 1543–1556. <https://doi.org/10.1002/ar.24263>
- Maes, C., Kobayashi, T., Selig, M.K., Torreken, S., Roth, S.I., Mackem, S. et al. (2010) Osteoblast precursors, but not mature osteoblasts, move into developing and fractured bones along with invading blood vessels. *Developmental Cell*, 19(2), 329–344. <https://doi.org/10.1016/j.devcel.2010.07.010>
- Matsuura, T., Tokutomi, K., Sasaki, M., Katafuchi, M., Mizumachi, E. & Sato, H. (2014) Distinct characteristics of mandibular bone collagen relative to long bone collagen: relevance to clinical dentistry. *BioMed Research International*, 2014, 769414. <https://doi.org/10.1155/2014/769414>
- Nakashima, K., Zhou, X., Kunkel, G., Zhang, Z., Deng, J.M., Behringer, R.R. et al. (2002) The novel zinc finger-containing transcription factor osterix is required for osteoblast differentiation and bone formation. *Cell*, 108(1), 17–29.
- Parada, C. & Chai, Y. (2015) Mandible and tongue development. *Current Topics in Developmental Biology*, 115, 31–58. <https://doi.org/10.1016/bs.ctdb.2015.07.023>
- Parada, C., Han, D. & Chai, Y. (2012) Molecular and cellular regulatory mechanisms of tongue myogenesis. *Journal of Dental Research*, 91(6), 528–535. <https://doi.org/10.1177/0022034511434055>
- Pauws, E., Hoshino, A., Bentley, L., Prajapati, S., Keller, C., Hammond, P. et al. (2009) Tbx22null mice have a submucous cleft palate due to reduced palatal bone formation and also display ankyloglossia and choanal atresia phenotypes. *Human Molecular Genetics*, 18(21), 4171–4179. <https://doi.org/10.1093/hmg/ddp368>
- Peng, Y., Wang, X.-H., Su, C.-N., Qiao, W.-W., Gao, Q., Sun, X.-F. et al. (2020) RNA-seq analysis of palatal transcriptome changes in all-trans retinoic acid-induced cleft palate of mice. *Environmental Toxicology and Pharmacology*, 80, 103438. <https://doi.org/10.1016/j.etap.2020.103438>
- Percival, C.J. & Richtsmeier, J.T. (2013) Angiogenesis and intramembranous osteogenesis. *Developmental Dynamics*, 242(8), 909–922. <https://doi.org/10.1002/dvdy.23992>
- Perez-Amodio, S., Jansen, D.C., Schoenmaker, T., Vogels, I.M.C., Reinheckel, T., Hayman, A.R. et al. (2006) Calvarial osteoclasts express a higher level of tartrate-resistant acid phosphatase than long bone osteoclasts and activation does not depend on cathepsin K or L activity. *Calcified Tissue International*, 79(4), 245–254. <https://doi.org/10.1007/s00223-005-0289-z>
- Pratap, J., Galindo, M., Zaidi, S.K., Vradii, D., Bhat, B.M., Robinson, J.A. et al. (2003) Cell growth regulatory role of Runx2 during proliferative expansion of preosteoblasts. *Cancer Research*, 63(17), 5357–5362.
- Quarto, N., Wan, D.C., Kwan, M.D., Panetta, N.J., Li, S.L. & Longaker, M.T. (2010) Origin matters: differences in embryonic tissue origin and Wnt signaling determine the osteogenic potential and healing capacity of frontal and parietal calvarial bones. *Journal of Bone and Mineral Research*, 25(7), 1680–1694. <https://doi.org/10.1359/jbmr.091116>
- Rakocevic, J., Orlic, D., Mitrovic-Ajtic, O., Tomasevic, M., Dobric, M., Zlatic, N. et al. (2017) Endothelial cell markers from clinician's perspective. *Experimental and Molecular Pathology*, 102(2), 303–313. <https://doi.org/10.1016/j.yexmp.2017.02.005>
- Rutkovskiy, A., Stensløkken, K.-O. & Vaage, I.J. (2016) Osteoblast differentiation at a glance. *Medical Science Monitor Basic Research*, 22, 95–106. <https://doi.org/10.12659/msmbr.901142>
- Santagati, F. & Rijli, F.M. (2003) Cranial neural crest and the building of the vertebrate head. *Nature Reviews Neuroscience*, 4(10), 806–818. <https://doi.org/10.1038/nrn1221>
- Shabtai, Y., Jubran, H., Nassar, T., Hirschberg, J. & Fainsod, A. (2016) Kinetic characterization and regulation of the human retinaldehyde dehydrogenase 2 enzyme during production of retinoic acid. *Biochemical Journal*, 473(10), 1423–1431. <https://doi.org/10.1042/BCJ20160101>
- Smith, T.M., Lozanoff, S., Iyyanar, P.P. & Nazari, A.J. (2012) Molecular signaling along the anterior-posterior axis of early palate development. *Frontiers in Physiology*, 3, 488. <https://doi.org/10.3389/fphys.2012.00488>
- Spiegelmaere, W.D., Cornillie, P., Casteleyn, C., Burvenich, C. & Broeck, W.V.D. (2010) Detection of hypoxia inducible factors and angiogenic growth factors during foetal endochondral and intramembranous ossification. *Anatomia Histologia Embryologia*, 39(4), 376–384. <https://doi.org/10.1111/j.1439-0264.2010.01005.x>
- Stein, G.S., Lian, J.B., Wijnen, A.J.V., Stein, J.L., Montecino, M., Javed, A. et al. (2004) Runx2 control of organization, assembly and activity of the regulatory machinery for skeletal gene expression. *Oncogene*, 23(24), 4315–4329. <https://doi.org/10.1038/sj.onc.1207676>

- Suzuki, A., Sangani, D.R., Ansari, A. & Iwata, J. (2016) Molecular mechanisms of midfacial developmental defects. *Developmental Dynamics*, 245(3), 276–293. <https://doi.org/10.1002/dvdy.24368>
- Svandova, E., Anthwal, N., Tucker, A.S. & Matalova, E. (2020) Diverse fate of an enigmatic structure: 200 years of Meckel's Cartilage. *Frontiers in Cell and Developmental Biology*, 8, 821. <https://doi.org/10.3389/fcell.2020.00821>
- Velasco, M.G., Ysunza, A., Hernandez, X. & Marquez, C. (1988) Diagnosis and treatment of submucous cleft palate: a review of 108 cases. *Cleft Palate-Craniofacial Journal*, 25(2), 171–173.
- Veselá, B., Švandová, E., Bobek, J., Lesot, H. & Matalová, E. (2019) Osteogenic and angiogenic profiles of mandibular bone-forming cells. *Frontiers in Physiology*, 10, 124. <https://doi.org/10.3389/fphys.2019.00124>
- Wang, L., Tang, Q., Xu, J., Li, H., Yang, T., Li, L. et al. (2020) The transcriptional regulator MEIS2 sets up the ground state for palatal osteogenesis in mice. *Journal of Biological Chemistry*, 295(16), 5449–5460. <https://doi.org/10.1074/jbc.RA120.012684>
- Weatherley-White, R.C., Sakura, C.Y., Brenner, L.D., Stewart, J.M. & Ott, J.E. (1972) Submucous cleft palate. Its incidence, natural history, and indications for treatment. *Plastic and Reconstructive Surgery*, 49(3), 297–304.
- Welsh, I.C. & O'Brien, T.P. (2009) Signaling integration in the rugae growth zone directs sequential SHH signaling center formation during the rostral outgrowth of the palate. *Developmental Biology*, 336(1), 53–67. <https://doi.org/10.1016/j.ydbio.2009.09.028>
- Xu, J., Huang, Z., Wang, W., Tan, X., Li, H., Zhang, Y. et al. (2018) FGF8 signaling alters the osteogenic cell fate in the hard palate. *Journal of Dental Research*, 97(5), 589–596. <https://doi.org/10.1177/0022034517750141>
- Xu, J., Wang, L., Li, H., Yang, T., Zhang, Y., Hu, T. et al. (2019) Shox2 regulates osteogenic differentiation and pattern formation during hard palate development in mice. *Journal of Biological Chemistry*, 294(48), 18294–18305. <https://doi.org/10.1074/jbc.RA119.008801>
- Yu, L., Gu, S.P., Alappat, S., Song, Y.Q., Yan, M.Q., Zhang, X.Y. et al. (2005) Shox2-deficient mice exhibit a rare type of incomplete clefting of the secondary palate. *Development*, 132(19), 4397–4406. <https://doi.org/10.1242/dev.02013>
- Yuan, Y. & Chai, Y. (2019) Regulatory mechanisms of jaw bone and tooth development. *Current Topics in Developmental Biology*, 133, 91–118. <https://doi.org/10.1016/bs.ctdb.2018.12.013>
- Zhang, Y.D., Chen, Z., Song, Y.Q., Liu, C. & Chen, Y.P. (2005) Making a tooth: growth factors, transcription factors, and stem cells. *Cell Research*, 15(5), 301–316. <https://doi.org/10.1038/sj.cr.7290299>
- Zhang, Z.Y., Song, Y.Q., Zhao, X., Zhang, X.Y., Fermin, C. & Chen, Y.P. (2002) Rescue of cleft palate in Msx1-deficient mice by transgenic Bmp4 reveals a network of BMP and Shh signaling in the regulation of mammalian palatogenesis. *Development*, 129(17), 4135–4146.

SUPPORTING INFORMATION

Additional Supporting Information may be found in the online version of the article at the publisher's website.

How to cite this article: Liao, C., Lu, M., Hong, Y., Mao, C., Chen, J., Ren, C., et al (2022) Osteogenic and angiogenic profiles of the palatal process of the maxilla and the palatal process of the palatine bone. *Journal of Anatomy*, 240, 385–397. <https://doi.org/10.1111/joa.13545>